Journal of Medicinal and Chemical Sciences 5 (2022) 1321-1330

Journal of Medicinal and Chemical Sciences

Journal homepage: http://www.jmchemsci.com/

Original Article (Special Issue)

Dielectric and Electrical Properties of Intercalated 1-(4-nitrophenyl)-*N*-(*p*-tolyl) methanimine into the Interlayers of Bentonite Clay

Ali J. A. Al-Sarray[1,*], Tarik Al-Kayat[2], Borhan Mustafa Mohammed[3], Mohammed Jassim Bader Al-assadi[4], Yousif Abu-Zaid[5]

[1]*Department of Chemistry, College of Science, University of Baghdad, Baghdad, Iraq*
[2]*Medical Technical College, Al-Farahidi Unviersity, Baghdad, Iraq*
[3]*Department of Medical Labs Technologies, Mazaya University College, Thi-Qar, Iraq*
[4]*Al-Maaqal University College, Basrah, Iraq*
[5]*Department of Chemistry, College of Education for pure sciences Ibn-Alhaitham, University of Baghdad, Baghdad, Iraq*

ARTICLE INFO

Article history
Receive: 2022-05-13
Received in revised: 2022-06-18
Accepted: 2022-08-22
Manuscript ID: JMCS-2207-1582
Checked for Plagiarism: **Yes**
Language Editor:
Dr. Fatimah Ramezani
Editor who approved publication:
Dr. Zeinab Arzehgar
DOI:10.26655/JMCHEMSCI.2022.7.21

KEYWORDS
Dielectric permittivity
Organo-clay complexes
Bentonite
Schiff base
Conductivity
Activation energy
Relaxation time

ABSTRACT

In this work, the dielectric properties of intercalated 1-(4-nitrophenyl)-N-(p-tolyl) methanimine into bentonite interlayers were investigated in the frequency range 10^2 to 10^6 Hz at five different temperatures between 24°C and 60°C. The impedance of the composite decreased with increasing the temperature from 24°C to 60°C, as it drops $7*10^3$ Ω at 100 Hz and $1.5*10^3$ Ω at 1 MHz. The composite showed a very low conductivity with little effect of increasing temperature in the low frequencies, yet the high frequencies make the effect of maximizing the temperature more obvious. The imaginary dielectric permittivity exhibited peaks of energy losses which reached the highest magnitude with 60°C, whereas the dielectric breakdowns were shifted toward higher frequencies with increasing temperature. Moreover, the activation energy of relaxation time was obtained by using Arrhenius equation from the slope of ln(τ) vs. $(KT)^{-1}$ curve and the value was (965.24 J). In the same approach, the activation energies of charge carriers were estimated in three different frequency regions; high, moderate, and low regions and the values were 529.31, 698.09, and 541.98 J, respectively.

GRAPHICAL ABSTRACT

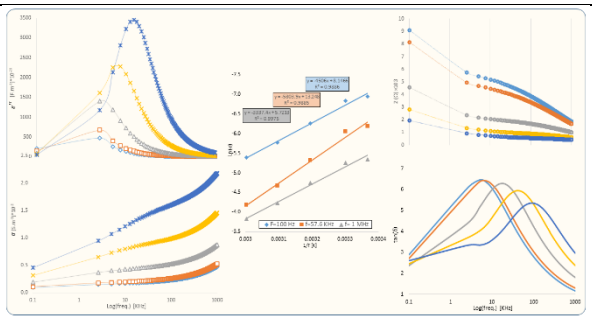

* Corresponding author: Ali J. A. Al-Sarray
✉ E-mail: Email: albaghdady1993@gmail.com

Introduction

Clay minerals and their complexes with organic species have captured considerable attention among researchers due to their mechanical, electrical, dielectric, and sensing properties. In addition, the intercalating abilities of these materials offer excellent possibilities in terms of altering their properties with inserting different organic and inorganic species within their interlayers [1]. Such properties enable the organo-clay composites for being promising materials for many applications. For instance, these composites can be used as a unique kind of memory storage materials due to their non-linear optical features and being spectral hole burning [2, 3]. The wide range of applications of these composites require an essential understanding to their electrical and dielectric properties [4].

However, Montmorillonite is one of the most clay minerals known, which is contained in different kinds of clays such as bentonite clay. The unit cells of these clay minerals are made of one octahedral alumina sheet located within two tetrahedral silica sheets to compose the layers of the clay mineral as unit cells. The spaces between these unit cells are filled with flooding inorganic ions and water molecules [5, 6].

One of the well-developed tool for separating the contributions of grain boundary from the total conductivity is the impedance spectroscopy, as this technique exhibits an electric response in a very wide frequency range [7]. The electric response represents the contribution of the motions of the charge carriers in the electric field, and these motions can be in different forms such as space charge formation, dipole reorientation, charge displacement, and other forms of motions [7-12].

On the other hand, studying the relationship between the frequency of the applied field and the dielectric loss factor can provide enough information to determine the relaxation time of material orientation momentum which in turn was used to calculate the activation energy of transition state time of charge carrier. Furthermore, the response of the charge carrier to the applied field takes very short time as in case of transition states [13]. Moreover, these transition states require certain energy to be maintained before being diminished which represent, in this case, the barrier energy. Furthermore, this barrier energy represents the activation energy required to change the state of material or its contents from the state of isolation to the state of conduction which supposed to be oriented toward the applied field.

Many studies had been carried out to investigate the electrical behavior of clay minerals and its complexes with organic species. Bore *et al.* [24] used a high frequency dielectric relaxation spectroscopy to estimate the interfacial water molecules on the clay interlayers, whereas belyaeva *et al.* [22] studied the saline soils by monitoring the complex dielectric permittivity at frequency 10 KHz to 8 GHz. Repin *et al.* [21] proposed a modeling approach to calculate the dielectric relaxation of different clay mentals at various temperatures.

The aim of this study is to investigate the effect of intercalating organic species, particularly Schiff base derivative, within the layer of montmorillonite clay minerals on the electrical and dielectric properties of the formed composite, as well as to estimate the activation energy of charge carriers and the relaxation time.

Experiments and Methods

Instrumental apparatus

A IM3570 model of Hioki impedance analyzer and LCR meter with frequency measurement range (4 Hz – 8 MHz) and delivering 0.05% rdg accuracy was used to estimate the dielectric properties of the prepared materials. In addition, the measurement range was between 100 mΩ and 100 MΩ with high accuracy mode (10Ω).

Preparing Samples for Dielectric Measurements

The powder of the samples prepared in our previous work [14] are compressed under 6-ton of pressure to shape them as disc pellets of 0.2 mm thickness and 15 mm diameter (±0.01 mm). The surface of both sides of the compressed pellets were coated with conducting silver paints, and then mounted between stainless-steel electrode plates which adjusted with a micro-screw. However, a guard ring was incorporated to the upper electrode to get rid of the current effects of

the edge and surface represented in forms of leakage currents that flowed on the surface of the samples and stray capacitance of the edges of the electrode. The diameter of the upper electrode is 10 mm, whereas the lower electrode has diameter around 30 mm. The upper electrode which incorporated by the guard rind is used to determine the effective volume of the sample.

Electrical and Dielectric Calculations

The complex permittivity, electrical impedance, and electrical conductivity are determined for all the prepared samples. As the complex dielectric permittivity is depending on the frequency of the applied field (ω=2πf) which can be derived directly from the complex capacitance [15], as demonstrated in Equation 1.

$$\varepsilon^*(\omega) = \frac{C^*(\omega)}{C_o} \quad (1)$$

Where, C^* represents the complex capacitance, C_o indicates the empty cell capacitance equal to $\varepsilon_{air}A/d$, d represents the thickness, and A is the area of the electrode.

The imaginary part of the dielectric permittivity, which represents the dielectric loss of the materials, is symbolized by ε" and the real part by ε'. The imaginary dielectric permittivity is comprised from contributions of the dc conductivity (σ_{dc}) and the relaxation processes [16], as described in Equation 2.

$$\varepsilon^* = \varepsilon' - i\left(\varepsilon''_{relax} + \frac{\sigma_{dc}}{\omega\varepsilon_0}\right) \quad (2)$$

Where, ε_0 is the vacuum permittivity with a value of 8.85*10-12 F/m.

The relaxation processes are usually identified by the dissipation factor (tanδ), as exhibited in Equation 3.

$$\tan\delta = \frac{\varepsilon''}{\varepsilon'} \quad (3)$$

There is a relation between the complex permittivity and the conductivity, as in Equation 4.

$$\sigma^* = i\omega\varepsilon_0\varepsilon^* \quad (4)$$

While the complex resistivity is related to the complex conductivity, as depicted in equation 5.

$$\rho^*(\omega) = \frac{1}{\sigma^*(\omega)} \quad (5)$$

The activation energies of the prepared materials were calculated by Arrhenius relation, as represented in Equation 6.

$$\sigma^* = \sigma_0 \exp\left(\frac{-E_a}{k_B T}\right) \quad (6)$$

Where, σ_0 is the pre-exponential factor, E_a is the activation energy, k_B is the Boltzmann constant, and T is the absolute temperature. Equation 6 was also used to calculate the activation energy for relaxation time through replacing σ^* with τ which represents the relaxation time of material.

Results and Discussion

Electrical Impedance Analysis

A typical impedance behavior was noticed for the prepared composite (Figure 1), where it is decreased with increasing of both temperature and frequency of the applied field. The effect of increasing the temperature can be attributed to increasing the kinetic energy of charge carriers [17]. A steep drop of electrical impedance occurs at low frequencies region with increasing the temperature which is similar to the general behavior of semiconductors. Nevertheless, a significant increase can be noticed at low temperatures with increasing the applied frequencies due to the low random motions of charge carriers which coincide with the applied field. Lower temperatures such as 24 °C and 30 °C show a higher impedance than that for higher temperatures, even in the higher frequency region which can be attributed to the restriction of new charge carriers and mismatch between its motions and the applied field [18].

Dielectric Loss

The spectrum of dielectric loss shows the regions of resonance with the applied field as bands with maximum values of losing energy (Figure 2). These peaks shift with increasing the temperature to the higher frequencies due to increasing of randomized kinetic energies added to the charge carriers. Thus, the motions of charge carriers coincide with higher frequencies with respect to increasing temperature. On the other hand, increasing the intensity of the peaks is noticed with increasing temperature attributed to the response of the charge carriers with the applied field. Unlike raw-bentonite clay [19], where the major charge carrier between layers of alumina-silica is calcium ion, in this composite calcium ion was constricted or eliminated by the protonated

organic compound within the layers. Moreover, the new charge carrier seems to be less affected by temperature and indicates a semi-stabilized resonance with the applied field [20].

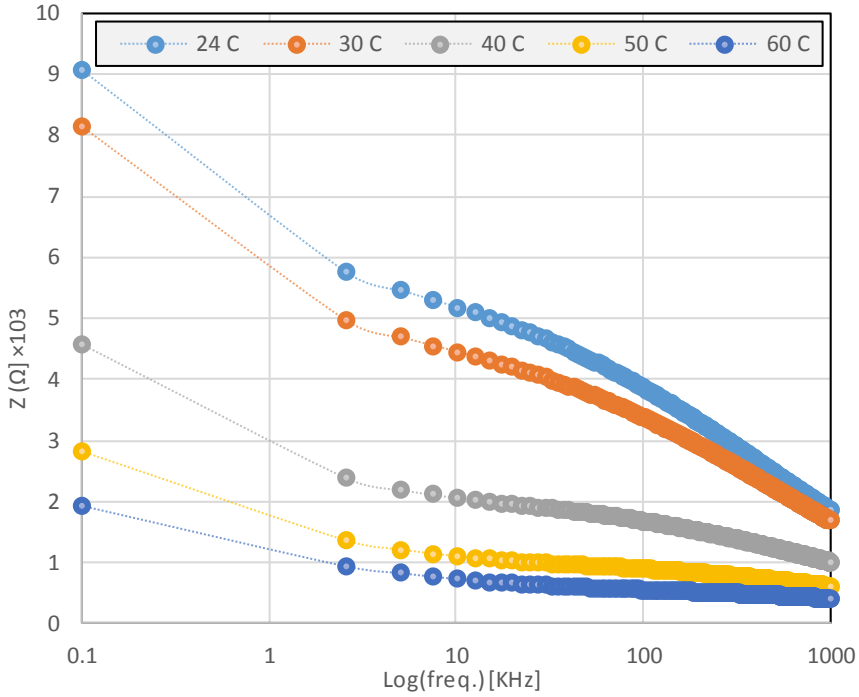

Figure 1: Impedance (Z) spectrum of the composite

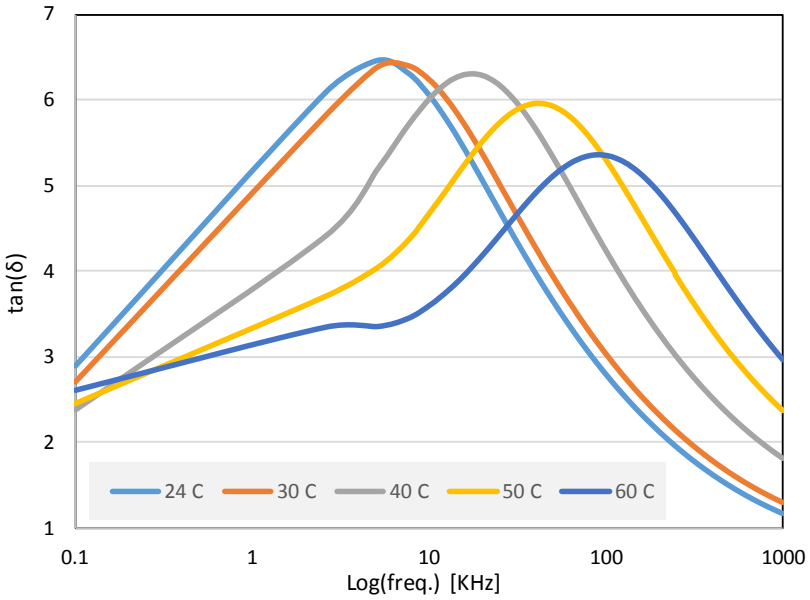

Figure 2: Dielectric loss (tanδ) spectrum of the composite

Dielectric Permittivity

In the spectrum of imaginary part of the dielectric permittivity (Figure 3), we can notice the magnitude change of peaks intensity of the composite with various temperatures compared to raw-bentonite [19]. At low temperatures (24-30°C), the intensity of the peaks where significantly low which indicate less adjustment between the frequency of applied field and the slow motion of the new charge carriers. Due to the steric effect of the intercalated organic molecule which somehow blocks the charge carrier movements, low temperatures could not provide enough energy to rotate or change the conformation of new organic substitution within bentonite layers to allow the charge carriers to have more freedom of motion [21]. However, at higher temperatures 40-60°C, the intensities are

noticeably higher due to higher energies provided by increasing the temperature and enough energy for rotating the organic conformation as well as reducing the constriction of charge carriers. Therefore, more losses of the applied field energy with increasing the temperature for the field to coincide with the movement of charge carriers [22].

However, the spectrum of real part of the dielectric permittivity (Figure 4) shows steep dropping of dielectric constant at low temperatures (24-30°C) right from the lower frequencies attributed to the disability of the applied field to coincide with the charge carrier movements due to the organic molecules which restrict the charge carrier movement. Nevertheless, linear behavior can be noticed at higher temperatures (40-60°C) which occur at low frequency region (100-5000 Hz). In addition, the breakdown of the dielectric constant happened at range of frequencies (5000-100000 Hz) as the resonance occurs between the applied field frequencies and the movement of the charge carrier. Moreover, the behavior of the dielectric constant starts to line up at higher frequencies due to the stability of the charge carriers with changing the applied field [23].

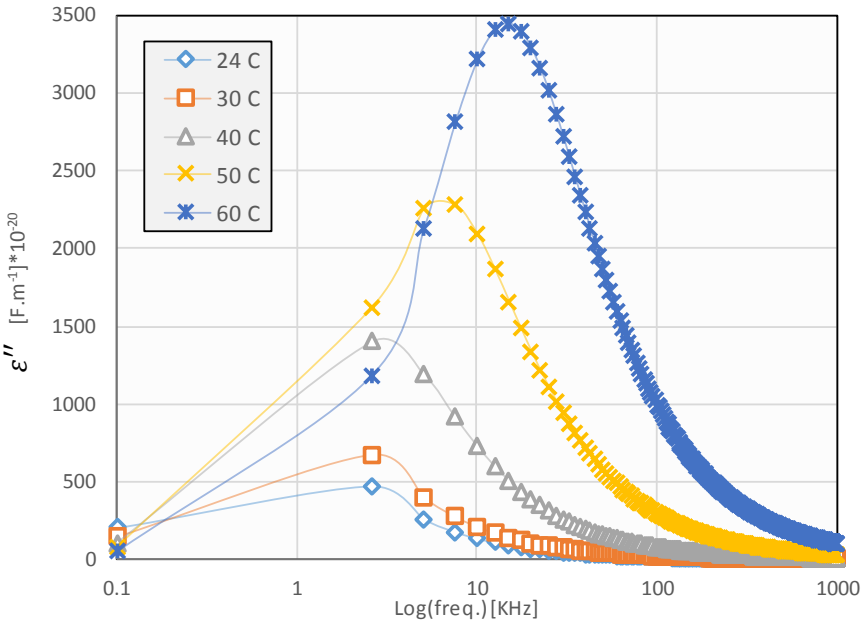

Figure 3: Spectrum of imaginary dielectric permittivity of the composite

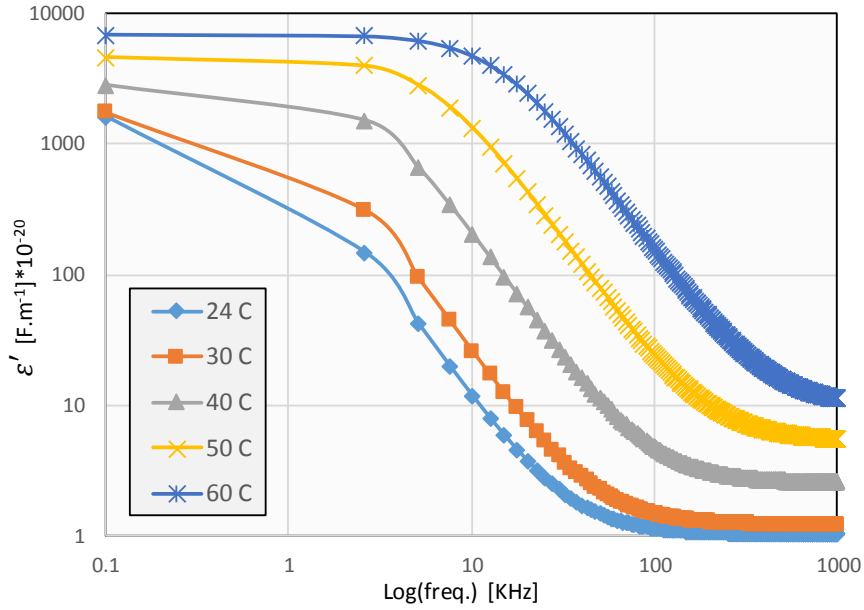

Figure 4: Spectrum of real dielectric permittivity of the composite

Electrical Conductivity Analysis

The behavior of conductivity of prepared composite (Figure 5) is somewhat similar to semiconductors as the increasing the temperature elevate the conductivity due to increasing the kinetic energy provided to the charge carrier to surpass the energy barrier of constricted environment. Moreover, the electrical conductivity changes with respect to the change of frequency representing the response extension of the material to the applied field. Because of the highly restricted environment, due to the presence of intercalated Schiff base molecule located in the pathway of charge carriers, low temperatures (24-30°C) do not have the ability to provide enough energy to rotate or re-orient the organic molecules to allow the ions to move freely.

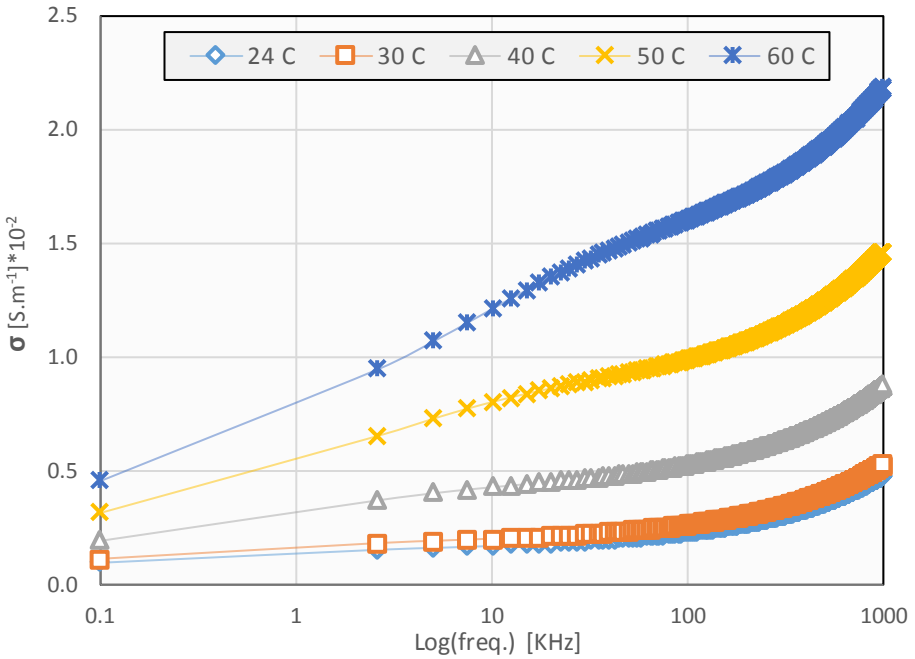

Figure 5: Conductivity spectrum of the composite

Activation Energies of Charge Carriers

The conductivity spectrum of the prepared composite was divided into three regions based on the values of frequencies, these regions are: low frequency region, moderate frequency region, and high frequency region, as listed in (Table 1). Furthermore, all of these regions obey the linearity of Arrhenius relationship when the conductivity is drawing against temperature (Figure 6). Hence, the activation energy of the charge carrier can be calculated for these three regions [24].

Table 1: Conductivity values of the composite in different frequency regions at different temperatures

Temp. [°C]	Conductivity at		
	f= 100 Hz	f= 57.6 KHz	f= 1 MHz
24	9.66E-04	2.06E-03	4.76E-03
30	1.08E-03	2.37E-03	5.23E-03
40	1.92E-03	4.92E-03	8.75E-03
50	3.13E-03	9.39E-03	1.46E-02
60	4.56E-03	1.52E-02	2.18E-02

Obviously, the environment of hydrogen bonding is considerably reduced when Schiff bases are formed in-between bentonite layers. Thus, most probably that charge carriers are more restricted

compared with the raw-bentonite. Furthermore, at low frequency region, the composite showed high values of activation energies and subsequently increasing the energy barrier indicating that the charge carrier is experiencing more restriction due to the presence of intercalated molecules. Most probably, the charge carrier which respond to the field should be impure protons which can move through the hydrogen bonding grid with water, aluminum, and silicon hydroxyls located within the crystal lattice of bentonite [25]. As a result of changing the charge carriers and being more restricted, it is reasonable for barrier energy to be elevated to reach the conductance state.

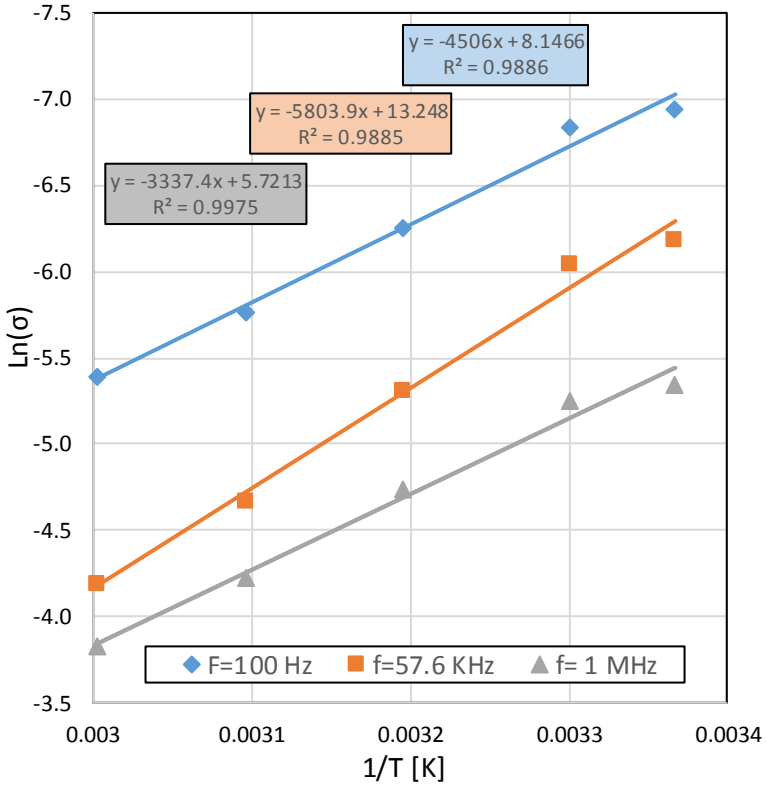

Figure 6: The linear representation of Arrhenius relation between conductivity and temperature

The region of response with the applied field included in the moderate frequency region showed a small reduction in the activation energy. This reduction can be interpreted as increasing the frequency of the field in this region that can secure less strained conformation of the organic molecules in order for the charge carrier ions to move with the field, and thus, achieving the state of conductance.

On the other hand, the activation energy values at a high frequency region indicated a significant reduction compared with the moderate and lower regions. Therefore, this reduction indicates that the main charge carrier is possessing a low moment of inertia which respond significantly to the high frequencies of the field. Moreover, this assures that the charge carrier which is responsible for the conductivity was changed to lighter ions which supposed to be the impure protons rather than calcium ions. Therefore, the hydrogen ion seems to be the only species which is capable of carrying the charges at these frequencies, while other species such as calcium ion and impurities are unable of carrying charges at this region (Figure 2).

Table 2: Activation energies of conductance state of the prepared composite

E_a [J]	Low frequency region	Moderate frequency region	High frequency region
PtoNB	541.98	698.09	529.31

Activation Energy of Relaxation Time

The activation energy of relaxation time for the composite was estimated by using Arrhenius relation (Figure 7) which was (965.24 J). This value is higher than that for raw bentonite attributed to the restriction which caused by the structures of the organic molecules which create a grid of hydrogen bonding with water and the environment of silicon-nitrogen dipoles. Thus, these restrictions of charge carrier responses elevate the barrier energy making this complex system has a shorter time of transition state than that of bentonite.

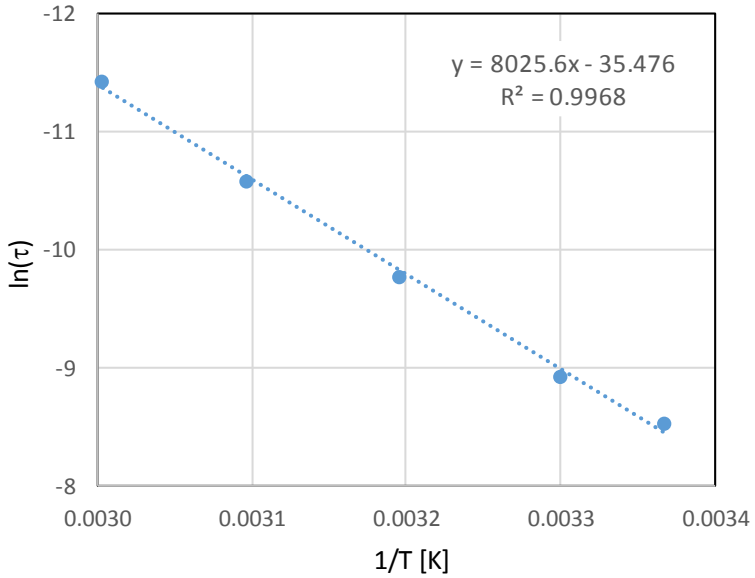

Figure 7: The linear representation of Arrhenius relation between relaxation time and temperature

Conclusion

The electrical and dielectric properties of the studied composite showed some distinctive features in terms of impedance, conductivity, and dialectic permittivity in the studied range of temperatures. The impedance range of the composite is $2*10^3$ -$9*10^3$ Ω in the studied temperatures, which higher than the pre-intercalated clay and that range drops significantly with increasing the frequency. The conductivity experienced the opposite way as its range was noticeably low and increased with raising the field. The dielectric losses revealed the behavior of the charge carriers with respect to the field and temperatures, whereas the dielectric breakdown shifted toward higher frequencies with increasing the temperature. The composite has the activation energy for the relaxation time equal to 965.24 J, with variant activation energy for the charge carriers based on the frequency regions.

Funding

This research did not receive any specific grant from funding agencies in the public, commercial, or not-for-profit sectors.

Authors' contributions

All authors contributed to data analysis, drafting, and revising of the paper and agreed to be responsible for all the aspects of this work.

Conflict of Interest

The author declared that they have no conflict of interest.

ORCID:

Ali J. A. Al-Sarray

https://www.orcid.org/0000-0001-6484-1763

References

[1]. Bergaya F., Lagaly G., General introduction: clays, clay minerals, and clay science, *Developments in clay science*, 2013, **5**:1 [Crossref], [Google Scholar], [Publisher]

[2]. Iwasaki M., Tai K., Okamoto M., Association of Quinocyanine Dyes under High Pressure, *Journal of the Society of Photographic Science and Technology of Japan*, 2002, **65**:291 [Crossref], [Google Scholar], [Publisher]

[3]. Okada T., Seki Y., Ogawa M., Designed nanostructures of clay for controlled adsorption of organic compounds, *Journal of Nanoscience and Nanotechnology*, 2014, **14**:2121 [Crossref], [Google Scholar], [Publisher]

[4]. Abollino O., Giacomino A., Malandrino M., Mentasti E., Interaction of metal ions with montmorillonite and vermiculite, *Applied Clay Science*, 2008, **38**:227 [Crossref], [Google Scholar], [Publisher]

[5]. Long L.H., Zhang Y.T., Wang X.F., Cao Y.X., Montmorillonite adsorbs urea and accelerates urea excretion from the intestine, *Applied Clay Science*, 2009. **46**:57 [Crossref], [Google Scholar], [Publisher]

[6]. Newton A.G., Lee J.Y., Kwon K.D., Na-montmorillonite edge structure and surface complexes: an atomistic perspective, *Minerals*, 2017, **7**:78 [Crossref], [Google Scholar], [Publisher]

[7]. Lvovich, V.F., *Impedance spectroscopy: applications to electrochemical and dielectric phenomena*, John Wiley & Sons, 2012 [Google Scholar], [Publisher]

[8]. Sati P.C., Kumar M., Chhoker S., Low temperature ferromagnetic ordering and dielectric properties of Bi1-xDyxFeO3 ceramics, *Ceramics International*, 2015, **41**:3227 [Crossref], [Google Scholar], [Publisher]

[9]. Gogoi P., Srinivas P., Sharma P., Pamu D., Optical, dielectric characterization and impedance spectroscopy of Ni-substituted MgTiO3 thin films, *Journal of Electronic Materials*, 2016, **45**:899 [Crossref], [Google Scholar], [Publisher]

[10]. Cao Z., Liu X., He W., Ruan X., Gao Y., Liu J., Extrinsic and intrinsic contributions for dielectric behavior of La2NiMnO6 ceramic, *Physica B: Condensed Matter*, 2015, **477**:8 [Crossref], [Google Scholar], [Publisher]

[11]. Coondoo I., Panwar N., Tomar A., Jha A.K., Agarwal S.K., Impedance spectroscopy and conductivity studies in SrBi2 (Ta1− xWx) 2O9 ferroelectric ceramics, *Physica B: Condensed Matter*, 2012, **407**:4712 [Crossref], [Google Scholar], [Publisher]

[12]. Lefi R., et al., Optical, electrical properties and characterization of (C2H5NH3) 2CdCl4 compound, *Optik*, 2016, **127**:5534 [Crossref], [Google Scholar], [Publisher]

[13]. Joshi J.H., Kanchan D.K., Joshi M.J., Jethva H.O., Parikh K.D., Dielectric relaxation, complex impedance and modulus spectroscopic studies of mix phase rod like cobalt sulfide nanoparticles, *Materials Research Bulletin*, 2017, **93**:63 [Crossref], [Google Scholar], [Publisher]

[14]. Al-Sarray A.J., Al-Mussawi I.M., Al-Noor T.H., Abu-Zaid Y., Organo-Clay Composites of Intercalated 4-Methylaniline and Its Schiff Base Derivative: Preparation and Characterization, *Journal of Medicinal and Chemical Sciences*, 2022, **5**:1094 [Crossref], [Google Scholar], [Publisher]

[15]. Kashir A., Jeong H.W., Lee G.H., Mikheenko P., Jeong Y., Dielectric properties of strained nickel oxide thin films, *Journal of the Korean Physical Society*, 2019, **74**:984 [Crossref], [Google Scholar], [Publisher]

[16]. Han T., Beloborodov R., Pervukhina M., Josh M., Cui Y., Zhi P., Theoretical modeling of dielectric properties of artificial shales, *Geofluids*, 2018, **2018**:2973181 [Crossref], [Google Scholar], [Publisher]

[17]. Elmelouky A., Mortadi A., Chahid E., Elmoznine R., Impedance spectroscopy as a tool to monitor the adsorption and removal of nitrate ions from aqueous solution using zinc aluminum chloride anionic clay, *Heliyon*, 2018, **4**:e00536 [Crossref], [Google Scholar], [Publisher]

[18]. Kiefer D., Yu L., Fransson E., Gómez A., Primetzhofer D., Amassian A., Campoy-Quiles M., Müller C., A solution-doped polymer semiconductor: insulator blend for thermoelectrics, *Advanced Science*, 2017, **4**:1600203 [Crossref], [Google Scholar], [Publisher]

[19]. Al-Sarray A.J., Al-Mousawi I.M.H., Al-Noor T.H., Acid Activation of Iraqi Bentonite Clay: Its Structural, Dielectric and Electrical Behavior at Various Temperatures. *Chemical Methodologies*, 2022, **6**:331 [Crossref], [Google Scholar], [Publisher]

[20]. Javaheri F., Esfandiarpour-Boroujeni I., Farpoor M.H., Holthusen D., Stewart R.D., Counterions, smectite, and palygorskite increase microstructural stability of saline-sodic soils, *Soil and Tillage Research*, 2022, **216**:105258 [Crossref], [Google Scholar], [Publisher]

[21]. Repin A.V., Rodionova O.V., Kroshka E.S., Modeling of Dielectric Relaxation in Clays at Negative and Positive Temperatures, *Russian Physics Journal*, 2021, **64**:67 [Crossref], [Google Scholar], [Publisher]

[22]. Belyaeva T., Bobrov P.P., Kroshka E.S., Repin A.V., Complex dielectric permittivity of saline soils and rocks at frequencies from 10 kHz to 8 GHz, In *2017 Progress In Electromagnetics Research Symposium-Spring (PIERS)*, IEEE, 2017, 3046-3051 [Crossref], [Google Scholar], [Publisher]

[23]. Csáki Š., Ondruška J., Trnovcova V., Štubňa I., Dobroň P., Vozár L., Temperature dependence of the AC conductivity of illitic clay, *Applied Clay Science*, 2018, **157**:19 [Crossref], [Google Scholar], [Publisher]

[24]. Bore T., Wagner N., Coperey A., Loewer M., Revil A., Scheuermann A., Analysis of Interfacial Water in Clay by High Frequency Dielectric Relaxation Spectroscopy, In: *2021 13th International Conference on Electromagnetic Wave Interaction with Water and Moist Substances (ISEMA)*, IEEE, 2021, 1 [Crossref], [Google Scholar], [Publisher]

[25]. Hatefi M., KomLakh K., Investigation of the effect of Duloxetine on pain status of patients with spinal cord injuries: A systematic review of drug therapy. *Eurasian Chemical Communications*, 2022, **4**:256 [Crossref], [Publisher]

HOW TO CITE THIS ARTICLE

Ali J. A. Al-Sarray, Tarik Al-Kayat, Borhan Mustafa Mohammed, Mohammed Jassim Bader Al-assadi. Yousif Abu-Zaid. Dielectric and Electrical Properties of Intercalated 1-(4-nitrophenyl)-*N*-(*p*-tolyl) methanimine into the Interlayers of Bentonite Clay. *J. Med. Chem. Sci*., 2022, 5(7) 1321-1330
https://doi.org/10.26655/JMCHEMSCI.2022.7.21
URL: http://www.jmchemsci.com/article_155240.html